



HAL
open science

Enhanced magnetization at the Cr/MgO(001) interface

M.-A. Leroy, A. M. Bataille, Qiang Wang, M. R. Fitzsimmons, F. Bertran, P. Le Fevre, A. Taleb-Ibrahimi, Adriana Vlad, A. Coati, Yves Garreau, et al.

► **To cite this version:**

M.-A. Leroy, A. M. Bataille, Qiang Wang, M. R. Fitzsimmons, F. Bertran, et al.. Enhanced magnetization at the Cr/MgO(001) interface. *Applied Physics Letters*, 2015, 107 (25), pp.251602. 10.1063/1.4938131 . hal-01707387

HAL Id: hal-01707387

<https://hal.science/hal-01707387>

Submitted on 5 Mar 2018

HAL is a multi-disciplinary open access archive for the deposit and dissemination of scientific research documents, whether they are published or not. The documents may come from teaching and research institutions in France or abroad, or from public or private research centers.

L'archive ouverte pluridisciplinaire **HAL**, est destinée au dépôt et à la diffusion de documents scientifiques de niveau recherche, publiés ou non, émanant des établissements d'enseignement et de recherche français ou étrangers, des laboratoires publics ou privés.

Enhanced magnetization at the Cr/MgO(001) interface

M.-A. Leroy, A. M. Bataille, Q. Wang, M. R. Fitzsimmons, F. Bertran, P. Le Fèvre, A. Taleb-Ibrahimi, A. Vlad, A. Coati, Y. Garreau, T. Hauet, C. Gatel, F. Ott, and S. Andrieu

Citation: *Appl. Phys. Lett.* **107**, 251602 (2015); doi: 10.1063/1.4938131

View online: <https://doi.org/10.1063/1.4938131>

View Table of Contents: <http://aip.scitation.org/toc/apl/107/25>

Published by the [American Institute of Physics](#)

Articles you may be interested in

[Anti-damping spin transfer torque through epitaxial nickel oxide](#)

Applied Physics Letters **106**, 162406 (2015); 10.1063/1.4918990

[Strain-induced modulation of perpendicular magnetic anisotropy in Ta/CoFeB/MgO structures investigated by ferromagnetic resonance](#)

Applied Physics Letters **106**, 072402 (2015); 10.1063/1.4907677

[Large enhanced perpendicular magnetic anisotropy in CoFeB/MgO system with the typical Ta buffer replaced by an Hf layer](#)

AIP Advances **2**, 032151 (2012); 10.1063/1.4748337

[Tunnel magnetoresistance of 604% at 300K by suppression of Ta diffusion in CoFeB / MgO / CoFeB pseudo-spin-valves annealed at high temperature](#)

Applied Physics Letters **93**, 082508 (2008); 10.1063/1.2976435

Scilight

Sharp, quick summaries **illuminating**
the latest physics research

Sign up for **FREE!**

AIP
Publishing



Enhanced magnetization at the Cr/MgO(001) interface

M.-A. Leroy,^{1,2} A. M. Bataille,^{1,a)} Q. Wang,^{3,b)} M. R. Fitzsimmons,^{3,c)} F. Bertran,⁴ P. Le Fèvre,⁴ A. Taleb-Ibrahimi,⁴ A. Vlad,⁴ A. Coati,⁴ Y. Garreau,^{4,5} T. Hauet,² C. Gatel,⁶ F. Ott,¹ and S. Andrieu²

¹Laboratoire Léon Brillouin, IRAMIS, CEA Saclay, 91191 Gif sur Yvette, France

²Institut Jean Lamour, Université de Lorraine, 54500 Vandœuvre les Nancy, France

³Los Alamos National Laboratory, Los Alamos, New Mexico 87545, USA

⁴Synchrotron SOLEIL, L'Orme des merisiers, 91192 Gif sur Yvette, France

⁵Matériaux et phénomènes quantiques (MPQ), Université Paris Diderot - Paris 7, Sorbonne-Paris-Cité, CNRS, UMR 7162, 10, rue A. Domon et L. Duquet 75205 Paris Cedex 13, France

⁶CEMES-CNRS, 29 rue Jeanne Marvig, 31055 Toulouse Cedex, France

(Received 31 August 2015; accepted 6 December 2015; published online 23 December 2015)

We report on the magnetization at the Cr/MgO interface, which we studied through two complementary techniques: angle-resolved photoemission spectroscopy and polarized neutron reflectivity. We experimentally observe an enhanced interface magnetization at the interface, yet with values much smaller than the ones reported so far by theoretical and experimental studies on Cr(001) surfaces. Our findings cast some doubts on the interpretations on previous works and could be useful in antiferromagnetic spin torque studies. © 2015 AIP Publishing LLC.

[<http://dx.doi.org/10.1063/1.4938131>]

In the field of spintronics, detailed knowledge of electronic and magnetic properties of interfaces is of the utmost importance to understand tunnel transport and exchange coupling mechanisms, particularly in fully epitaxial heterostructures like Fe/MgO/Fe (001).¹ In this system, the symmetry dependent attenuation rate of the MgO barrier favors the electronic transport by electrons with Δ_1 symmetry.² Chromium is also an interesting *bcc* metal for these symmetry conserving model systems: although the band structure of Cr differs only slightly from that of Fe, it possesses no Δ_1 bulk band at the Fermi level. It can hence be used as a spin filter for this electronic symmetry,^{1,3,4} and we have recently demonstrated a tunnel-mediated coupling in Cr/MgO/Cr systems⁵ similar to the one observed in Fe/MgO/Fe. The study of the antiferromagnetic ordering of Cr thin films and their interface magnetic properties are interesting for spin transfer torque (STT) in antiferromagnetic layers, which could compare favorably to the case of ferromagnetic tunnel junctions in terms of critical current, precession frequencies, or stray field.⁶ If present, non-compensated interface moments would generate a ferromagnetic-like contribution, which could dominate STT,⁷ and hence reduce the gain compared to ferromagnets.

As bulk material and in the bulk of thin films, Cr possesses a staggered magnetization with collinear magnetic moments. In the unstrained defect-free material, a magnetization modulation incommensurate with the structural lattice is observed, the so-called spin density wave (SDW) phase.⁸ The magnetic moments within the Cr(001) surface are ferromagnetically aligned and antiferromagnetically aligned with those of the following sub-surface layer.^{9–14} Several calculations of surface density of states^{9,10,15–17}

predict an enhancement of the surface moment (up to 3 μ_B /Cr atom), which reduces back to the unperturbed bulk value within about 6 layers.

To experimentally test these predictions, several groups have investigated the surface electronic states of Cr.^{18–22} Measurement of the exchange splitting of the surface states by the ferromagnetic surface enables the surface moment to be inferred.^{9,18,19} Band structure calculations in the Δ direction of the Cr Brillouin zone generally predict the existence of a filled majority surface state situated 1 eV below the Fermi energy E_F , and of a minority surface state near the Fermi level (filled or empty state), but the binding energies of these states vary largely according to the calculation method used.^{9,17–19,23}

Through angle resolved photoemission spectroscopy (ARPES), Klebanoff *et al.*¹⁸ have detected features situated, respectively, at 0.08 eV and 0.63 eV below the Fermi level that they interpreted as surface states. Assigning the first feature to a minority surface state and the second one to a majority surface state, they deduce a surface moment of 2.4 μ_B /Cr atom.²⁴ Later, Nakajima *et al.* found that the second feature situated at 0.63 eV below E_F was dispersive, and therefore a bulk state, hence putting in doubt the value of the surface magnetic moments previously derived by other groups.

Using STM spectroscopy, Stroschio *et al.* detected a similar feature at small voltage (–50 mV) that they attributed to a filled minority surface state.¹⁹ They deduced a smaller value of surface moment (1.7 μ_B /Cr atom) than that derived in earlier calculations. The symmetry of this feature is still controversial: ARPES^{18,25} and some spin-polarized STM studies^{20,26} agree on a Δ_1 symmetry, characteristic of a Shockley-type surface state, whereas other studies²⁰ suggest an orbital Kondo resonance with Δ_5 symmetry. Further compounding interpretation, the measured binding energy of this surface depends upon sample,^{19–21} which suggests an extrinsic origin, possibly defects or surface impurities.^{27,28}

^{a)}alexandre.bataille@cea.fr

^{b)}Present address: Materials Science Division, Argonne National Laboratory, Argonne, Illinois 60439, USA.

^{c)}Present address: Quantum Condensed Matter Division, Oak Ridge National Laboratory, Oak Ridge, Tennessee 37831, USA.

The studies mentioned above solely concern the electronic states of a bare Cr(001) surface, and the persistence of these polarized states at Cr/MgO interface has not yet been addressed. In this paper, we complete our previous work on the Cr electronic structure²⁵ and tackle the issue of the determination of interface magnetic moments. For this purpose, we employ complementary probes of magnetic structure, ARPES and polarized neutron reflectivity (PNR).²⁹

The ARPES measurements on a Cr surface and a Cr/MgO interface were carried out on the Cassiopée beamline at the synchrotron Soleil, the dedicated samples being grown *in-situ* through a process described in details elsewhere.²⁵ The thickness of the MgO overlayer has been evaluated to be 1.2 monolayer (ML) by comparing the intensity of the Mg 2*p* and Cr 3*p* core levels peaks measured by *in-situ* X-ray photoemission spectroscopy (XPS).³⁰ The angular precision of the ARPES setup was 0.1°, and the angular acceptance of the analyzer ±13°. The measurements have been performed with photon energy varying between 20 and 120 eV, with a 0.5 eV step, and the data have been interpolated using the standard processes in order to analyze the data in the reciprocal space.

The photoemission results most relevant for the present study are displayed in Figure 1. Since we have used a wide range of incident photon energies, and two light polarizations, we are able to distinguish between bulk and surface/interface states, and between the bands with Δ_1 (*s*, *p_z*, *d_{z²}* orbitals) or Δ_5 symmetry (*p_x*, *p_y*, *d_{xz}*, *d_{yz}* orbitals). All the peaks in Figure 1 can thus be ascribed to three features: first, a Δ_5 bulk band located at 0.67 eV below the Fermi level at the Γ point which dispersion along the normal Δ direction is in good agreement

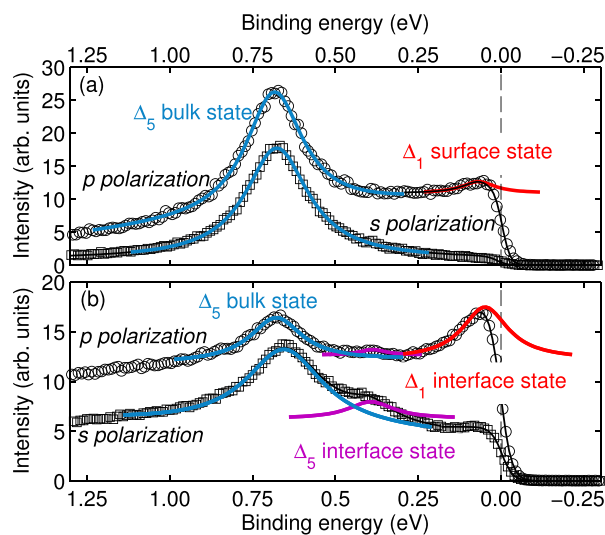


FIG. 1. Photoemission spectrum at the Γ point recorded in both polarizations, at $T = 150$ K. The data were recorded both for *s* polarization (\square) and for *p* polarization (\circ). All solid lines refer to fits of the data, either with pseudo-Voigt functions for the peaks, and a Fermi edge with an effective temperature of 200 K consistent with the actual temperature of the measurements, and the energy resolution, which is around 10 meV. The data presented here have been interpolated to provide data exactly at the Γ point, and corresponds to photon energies between 60 and 65 eV. (a) Cr(001) surface: two main features are visible, accounting for a bidimensional Δ_1 state and a bulk Δ_5 state. A Δ_5 surface state is also present²⁵ but not visible because of the too low cross section at this incident beam energy. (b) Cr/MgO interface: the two features observed for the Cr bare surface are still present, without noticeable change in their energy positions. A third feature situated at an intermediate binding energy is visible and corresponds to another interface state of Δ_5 symmetry.²⁵

with previous experimental investigations^{22,31} and with the calculations for the Cr Δ_5 bulk state.²⁵ We also observe two surface/interface states: one with the Δ_5 symmetry located around 0.4 eV below E_F , and another one with Δ_1 symmetry close to E_F (binding energy is 51 ± 10 meV for the surface state and 59 ± 11 meV for the interface state). No dispersion along the normal Δ direction is observed for these two states, which also exhibit the very same in-plane dispersion whatever the normal wavevector component.²⁵ This is characteristic of bidimensional states.

The relative intensities of the peaks differ largely between the two types of samples: the interface states are much less attenuated by the MgO overlayer than the bulk states, which may originate from the different escape depths (4 Å for the bare Cr sample compared to 2.5 Å for the Cr/MgO sample²⁵): the chromium “effective thickness” contributing to the bulk photoemission signal is much smaller in the case of the Cr/MgO sample, as is evidenced by the ratio between the Fermi edge and the bulk Δ_5 peak intensities observed with *s* polarization. Indeed, the Δ_5 surface state is not visible here given the large intensity of the bulk Δ_5 peak, but it has been observed in other region of the reciprocal space in our detailed study.²⁵ The most relevant conclusion of our electronic structure study regarding this paper is that the two samples are in fact very similar, since the *positions* of the different peaks are barely affected by the deposition of MgO. In particular, the energy shift between the Δ_1 surface and interface states is within the error bar. Moreover, the binding energy of these Δ_1 state is consistent to those observed by STM on clean Cr surfaces,^{20,26} so our sample allows us to draw conclusions on the intrinsic properties of Cr.

This has a very important consequence: given the intimate link between surface/interface magnetism and electronic structure, any result obtained by an *ex situ* technique on the magnetic moment at the Cr/MgO interface can be extended to the Cr(001) surface. Such a measurement would be truly intrinsic of Cr(001) since earlier studies^{18–20,22} report similar peak *positions* as in the present study (the discrepancies on the interpretation of the results comes from the lower energy resolution and/or the lack of symmetry resolution of the previous measurements). Our ARPES results look inconsistent with theoretical predictions which place the Δ_1 state about 1 eV above the Fermi level,^{16,17,23} corresponding to a magnetic moment of 2.3–3 μ_B /Cr atom. Making the same assumptions as Stroscio *et al.*,¹⁹ this leads to a value of 1.7 μ_B /Cr atom, but this estimation is model-dependent, which is a problem in the case of Cr (a notoriously difficult case for theoretical studies). To provide a quantitative and more direct measurement of the surface/interface moment, we performed PNR experiments.

We have grown by molecular beam epitaxy (MBE) a [Cr/MgO]₅ superlattice dedicated to PNR: the Cr and MgO thicknesses were chosen so as to maximize the magnetic signal from Cr/MgO interfaces. The epitaxial stack was deposited on a MgO(001) substrate. Each Cr layer was grown at room temperature and subsequently annealed at 650 °C to improve its crystallinity and decrease its surface roughness. The growth of each of the 10 MgO monolayers at room temperature was monitored using Reflection High Energy

Electron Diffraction (RHEED). XPS does not show any sign of Cr oxidation after MgO deposition and annealing at 650 °C even for a 1ML Cr layer.³⁰ High resolution Transmission Electron Microscope (TEM) micrographs of the superlattice do not reveal any parasitic phase at interfaces (Figures 2(a) and 2(b)). The micrographs confirm the continuity of the atomic columns throughout the stack and the low roughness of interfaces at atomic scale. In Figure 2(c), the existence of oscillations of the X-ray reflectivity up to at least the 22nd order is also evident for the high quality of the superlattice.

To study the volume magnetic ordering of the Cr layers included in the superlattice, we have exploited the sensitivity of neutron diffraction,³² using the 6T2 diffractometer at the LLB/Orphée neutron source in Saclay (France). The magnetic phase of the layer can be readily determined from the presence or absence of satellites peaks around two structurally forbidden Bragg reflections.⁵ Figure 3 displays reciprocal space maps recorded around the 001 Bragg position with $\lambda = 2.35 \text{ \AA}$. At 80 K, we only observe an $0\ 0\ 1+\delta$ peak (the $0\ 0\ 1-\delta$ peak is hidden by a parasitic peak at $0\ 0\ 0.955$), which is a unique signature of a transverse SDW phase spins lying in the film plane.⁵ As shown in Figures 3(b) and 3(c), the sample undergoes an incommensurate/commensurate transition with heating and is in a fully commensurate state at 300 K. Yet the spins remain in the film plane through the transition, so the domain structure and its alteration by an external magnetic field is expected to be similar on the whole temperature range.

The magnetization depth profile of the $[\text{Cr}/\text{MgO}]_5$ superlattice was measured with PNR using the Asterix reflectometer (a reflectometer using a pulsed neutron source with neutron wavelengths between 4 and 12 Å) at the Los Alamos Neutron Science Center, USA. Indeed, in both magnetic phases (commensurate and incommensurate) observed in our samples, the SDW polarization can be either along the a or b direction of the unit cell, and the energy cost of forming spin domains is small.^{33–35} In its virgin state, the sample is expected to be an even mix of the 4 possible domains (two possible directions for the interface moment for each SDW polarization). The field required to switch the polarization domains is about 20 kOe for bulk Cr³⁶ and larger for

epitaxial thin films,³⁷ with switching still not complete under 135 kOe,³⁸ so large fields were applied during the PNR measurements to favor a polarization domain as much as possible. The temperature was varied between 10 and 300 K.

Figure 4 displays a typical example of results, obtained at 80 K and under a 110 kOe magnetic field applied along the a direction, which favors spins aligned with the b direction.³⁶ The non-spin-flip reflectivities $I_{\uparrow\uparrow}$ and $I_{\downarrow\downarrow}$ appear very similar on Figure 4(a), yet a statistically significant asymmetry ($I_{\uparrow\uparrow} - I_{\downarrow\downarrow}/I_{\uparrow\uparrow} + I_{\downarrow\downarrow}$) is observed. The asymmetry curves exhibits two important features: a significant asymmetry on the superlattice peaks (Q around 0.37 and 0.75 nm^{-1} , grey shaded areas on Figure 4(a)), and fast asymmetry oscillations close to the reflectivity plateau.

According to the theoretical calculations, the envelope of the magnetization is expected to decay exponentially with the distance to the surface.¹⁰ Taking into account the staggered magnetization, this leads to a non-zero averaged moment on the last 7 atomic planes, which is the parameter we determined since the Q range covered by our PNR measurements is not large enough to allow atomic plane-resolution. Each Cr layer is thus cut into three slabs: the upper and lower nm (or last 7 Cr planes), in contact with the MgO layers, corresponding to the interfaces, while the remainder of each Cr layer is considered as bulk of the layers (see Figure 4(b)). The structural parameters (thickness and roughness) are fixed to the values obtained from the X-ray reflectivity measurements, and each Cr layer is considered as magnetically identical so the model only has two parameters: the averaged interface magnetization M_I and the bulk magnetization M_B , corresponding to a possible canting of Cr spins. The calculated spin asymmetry was found to be independent from the fine-tuning of the thickness and roughness of each individual layer of the superlattice. We first compared the measured asymmetry with the surface moments already reported from theoretical^{9,10,15–17} and experimental^{19,24} investigation. As shown in Figure 4(c), the calculated asymmetry far exceeds the measured one. A smaller value of M_I reproduces well the asymmetry at the superlattice peak positions (blue zones in Figure 4(d)) the amplitude of the small Q oscillations is underestimated. We also examined the possibility of a homogeneous

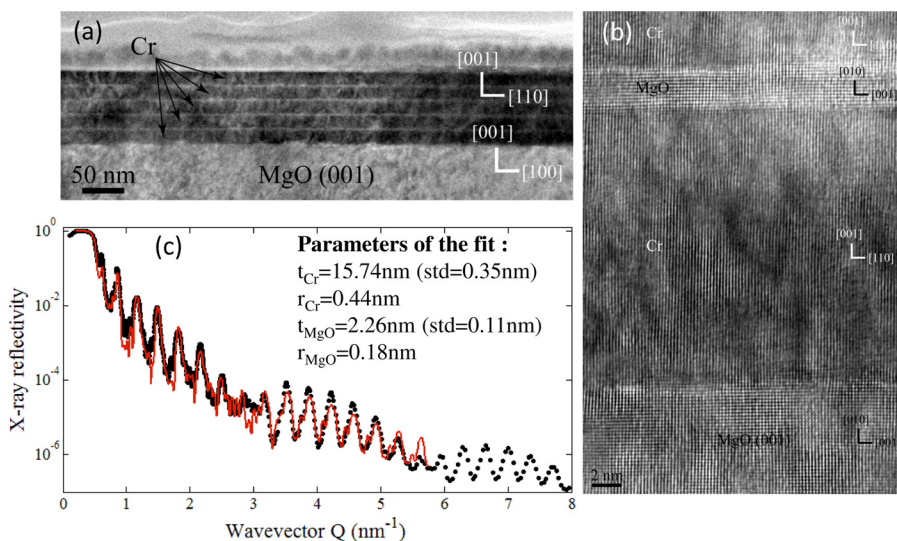


FIG. 2. (a) Low resolution Transmission Electron Microscope (TEM) micrograph of the $[\text{Cr}/\text{MgO}]_5$ superlattice. (b) High resolution micrograph showing the low local roughness of the interfaces and the continuity of atomic columns. (c) X-ray reflectivity curve measured on the SIXS beamline at the Soleil synchrotron, and physical parameters for the superlattice deduced from the fit (mean thicknesses t_{Cr} and t_{MgO} , roughnesses r_{Cr} and r_{MgO}), and their standard deviation for the five repetitions of the stack.

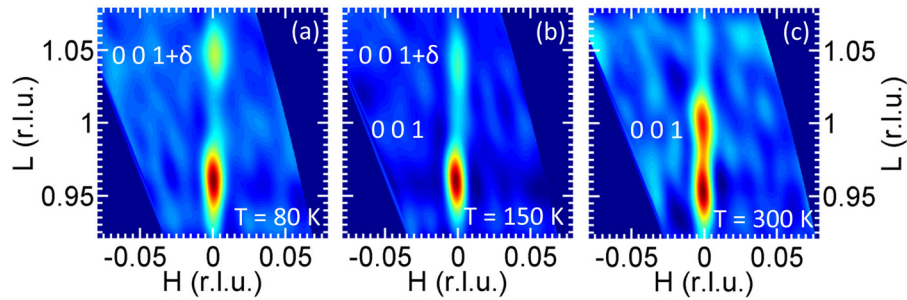


FIG. 3. Reciprocal space map around the 001 Bragg position. (a) $T = 80$ K. The $001 + \delta$ satellite evidences an incommensurate transverse incommensurate spin density wave phase with spins lying in plane. The extra intensity near the $001 - \delta$ position is a parasitic signal coming from the MgO substrate. (b) $T = 150$ K: some intensity is observed at 001, which corresponds to the apparition of a commensurate phase. (c) $T = 300$ K: the sample is now fully in its commensurate phase, with all the magnetic intensity in the 001 peak.

magnetization within the whole sample. As evidenced in Figure 4(e), this model reproduces quite well the fast asymmetry oscillations at low Q (green shaded zone), but not the spin asymmetry of the superlattice peaks. Eventually, the best model is a combination of the two scenarios (Figure 4(f)), with an interface magnetization much smaller than expected. We observe this enhanced moment on the whole temperature range, with a small temperature evolution: the high

temperature moment is about 50% larger than the moment at 80 K, which we ascribe to the broad phase transition undergone by our sample evidenced in Figure 3. Zero field measurements were performed at 150 and 200 K; a small (roughly 5 fold reduction compared to the 110 kOe measurements), but statistically significant spin asymmetry was observed at the superlattice peak in both cases, which indicates the presence of remanent interfacial magnetization.

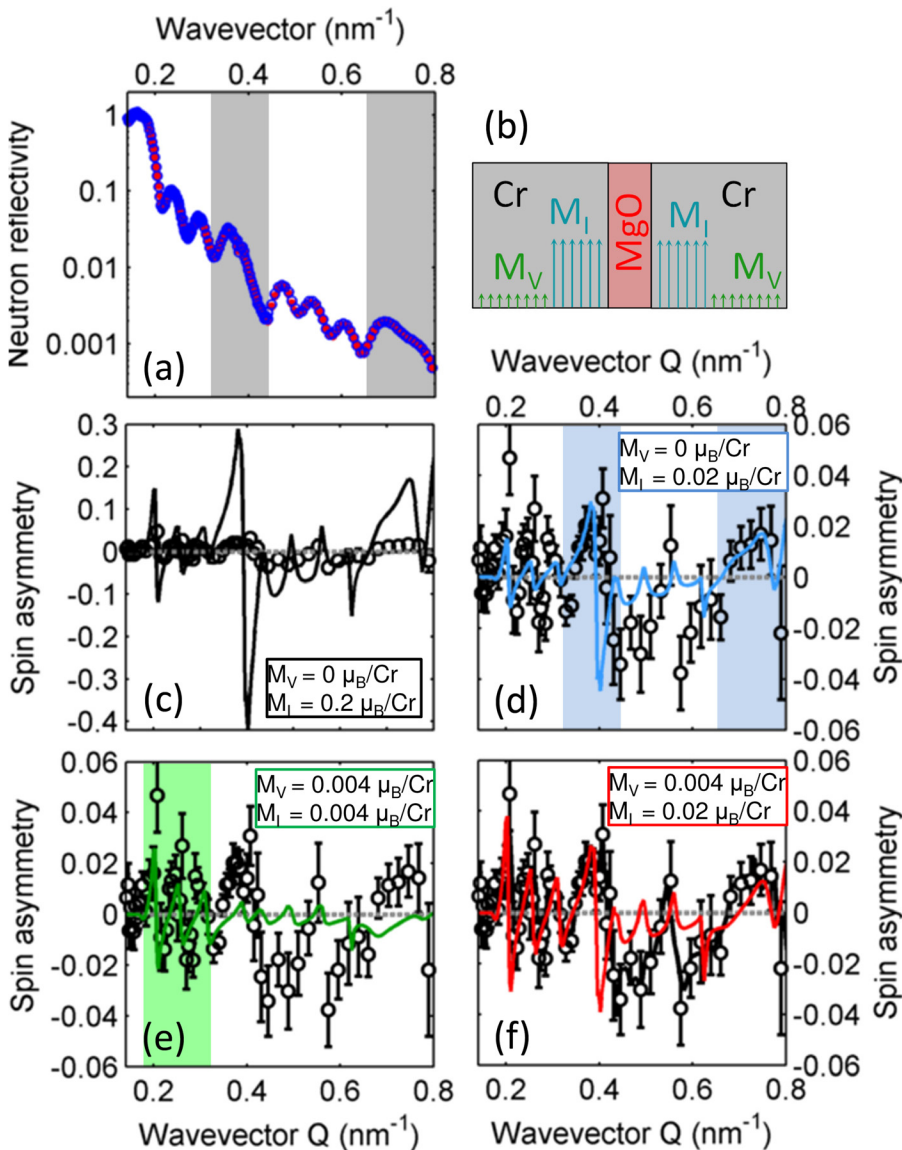


FIG. 4. (a) Polarized Neutron Reflectivity signal of the $[\text{Cr}/\text{MgO}]_5$ superlattice at 80 K and 110 kOe. The grey shaded areas correspond to the first and second superlattice peaks. (b) Schematic representation of the model with the two parameters used to reproduce the data: the volume magnetization M_V and the interface magnetization M_I . (c) Experimental spin asymmetry, compared with the signal calculated for a purely interfacial magnetization $M_I = 0.2 \mu_B/\text{Cr}$ atom corresponding to $2 \mu_B/\text{Cr}$ atom on the last Cr planes, a value similar to those already reported theoretically and experimentally. (d) Same as c, but with $M_I = 0.02 \mu_B/\text{Cr}$ atom. The agreement is rather good on the superlattice peaks (blue areas) but the model fails to reproduce the sharp oscillations at low Q accurately. (e) Comparison with the signal calculated for a homogeneous magnetization ($M_I = M_V = 0.004 \mu_B/\text{Cr}$ atom). Note that a homogeneous magnetization produces almost no asymmetry on the superlattice peaks, and only significantly contributes to low Q oscillations (green area). (f) Experimental spin asymmetry compared to a mixed model, with both a small volume contribution ($0.004 \mu_B/\text{Cr}$ atom) and an interface contribution ($0.02 \mu_B/\text{Cr}$ atom), which best reproduce our data.

Both the interfacial and bulk magnetization are very small: since the mean magnetic moment in the SDW phase is $0.4 \mu_B/\text{Cr}$ atom, the canting angle is less than one degree. Moreover, the theoretical calculations correspond to a value of $0.2 \mu_B/\text{Cr}$ atom for the magnetization averaged on the last nm of the Cr layer, which is 10 times larger than the value we obtain. Since the interface states of the Cr/MgO(001) system are very similar to the surface states of the Cr(001) surface, our conclusions on the former system hold for the latter, and the surface moment of Cr(001), while enhanced, is much lower than previously reported.

In summary, we have shown the presence of an enhanced magnetization at the Cr/MgO interface. To do so, we used two complementary techniques: high-resolution polarized neutron reflectivity allowed us to quantify the existence of the enhanced interface magnetization. The value of the interface moment is much smaller than expected from theoretical calculations and previous results reported on the magnetization of the Cr (001) surface. High-resolution angle-resolved photoemission gave us indirect insight on the magnetism at the Cr/MgO interface, through the position of the Δ_1 interface state very close to the Fermi level, which is fully consistent with the small value given by PNR. Since this position is little different for the Cr(001) surface state, our findings can be extended to the Cr surface and describe an intrinsic property of Cr(001). This questions the values of Cr(001) surface magnetization theoretically predicted or experimentally inferred from indirect methods. Our results also demonstrate that heterostructure comprising an epitaxial Cr/MgO bilayer (for example, a Cr/MgO/Fe trilayer) are good candidates to study the truly antiferromagnetic STT since the ferromagnetic-like contribution should be minimal.

We thank Amina Neggache for her help with the ARPES experiment and samples growth and Florence Porcher for her help during diffraction experiments. This work was supported by the French Agence Nationale de la Recherche, ANR-11-JS10-005 “Electra”. The HRTEM experiments were supported by the METSA network. This work has benefited from the use of the Lujan Neutron Scattering Center at LANSCE, which is funded by the Department of Energy’s Office of Basic Energy Science.

¹C. Tiusan, F. Greullet, M. Hehn, F. Montaigne, S. Andrieu, and A. Schuhl, *J. Phys.: Condens. Matter* **19**, 165201 (2007).

²W. H. Butler, X.-G. Zhang, T. C. Schulthess, and J. M. MacLaren, *Phys. Rev. B* **63**, 054416 (2001).

³R. Matsumoto, A. Fukushima, K. Yakushiji, S. Nishioka, T. Nagahama, T. Katayama, Y. Suzuki, K. Ando, and S. Yuasa, *Phys. Rev. B* **79**, 174436 (2009).

⁴T. Nagahama, S. Yuasa, E. Tamura, and Y. Suzuki, *Phys. Rev. Lett.* **95**, 086602 (2005).

⁵M.-A. Leroy, A. M. Bataille, B. Dkhil, F. Porcher, A. Barbier, V. L. R. Jacques, Y. Lu, C. Bellouard, T. Hauet, S. Ravy, J. Herrero-Martin, C. Gatel, K. Bouzehouane, A. Gukasov, S. Andrieu, and C. Tiusan, *Phys. Rev. B* **90**, 035432 (2014).

⁶H. V. Gomonay, R. V. Kunitsyn, and V. M. Loktev, *Phys. Rev. B* **85**, 134446 (2012).

⁷P. M. Haney, D. Waldron, R. A. Duine, A. S. Núñez, H. Guo, and A. H. MacDonald, *Phys. Rev. B* **75**, 174428 (2007).

⁸E. Fawcett, *Rev. Mod. Phys.* **60**, 209 (1988).

⁹G. Allan, *Surf. Sci.* **74**, 79 (1978).

¹⁰D. R. Grempel, *Phys. Rev. B* **24**, 3928 (1981).

¹¹S. Bluegel, D. Pescia, and P. H. Dederichs, *Phys. Rev. B* **39**, 1392 (1989).

¹²M. Kleiber, M. Bode, R. Ravlić, and R. Wiesendanger, *Phys. Rev. Lett.* **85**, 4606 (2000).

¹³T. Kawagoe, Y. Suzuki, M. Bode, and K. Koike, *J. Appl. Phys.* **93**, 6575 (2003).

¹⁴J. Lagoute, S. L. Kawahara, C. Chacon, V. Repain, Y. Girard, and S. Rousset, *J. Phys.: Condens. Matter* **23**, 045007 (2011).

¹⁵R. H. Victora and L. M. Falicov, *Phys. Rev. B* **31**, 7335 (1985).

¹⁶C. L. Fu and A. J. Freeman, *Phys. Rev. B* **33**, 1755 (1986).

¹⁷H. Hasegawa, *J. Phys. F: Met. Phys.* **16**, 1555 (1986).

¹⁸L. E. Klebanoff, R. H. Victora, L. M. Falicov, and D. A. Shirley, *Phys. Rev. B* **32**, 1997 (1985).

¹⁹J. A. Stroschio, D. T. Pierce, A. Davies, R. J. Celotta, and M. Weinert, *Phys. Rev. Lett.* **75**, 2960 (1995).

²⁰T. Hänke, M. Bode, S. Krause, L. Berbil-Bautista, and R. Wiesendanger, *Phys. Rev. B* **72**, 085453 (2005).

²¹O. Yu. Kolesnychenko, G. M. M. Heijnen, A. K. Zhuravlev, R. de Kort, M. I. Katsnelson, A. I. Lichtenstein, and H. van Kempen, *Phys. Rev. B* **72**, 085456 (2005).

²²N. Nakajima, O. Morimoto, H. Kato, and Y. Sakisaka, *Phys. Rev. B* **67**, 041402 (2003).

²³P. Habibi, C. Barreteau, and A. Smogunov, *J. Phys.: Condens. Matter* **25**, 146002 (2013).

²⁴L. E. Klebanoff, S. W. Robey, G. Liu, and D. A. Shirley, *Phys. Rev. B* **30**, 1048 (1984).

²⁵M.-A. Leroy, A. M. Bataille, F. Bertran, P. Le Fèvre, A. Taleb-Ibrahimi, and S. Andrieu, *Phys. Rev. B* **88**, 205134 (2013).

²⁶M. Budke, T. Allmers, M. Donath, and M. Bode, *Phys. Rev. B* **77**, 233409 (2008).

²⁷M. Schmid, M. Pinczolis, W. Hebenstreit, and P. Varga, *Surf. Sci.* **377**, 1023 (1997).

²⁸H. Oka and K. Sueoka, *J. Appl. Phys.* **99**, 08D302 (2006).

²⁹M. R. Fitzsimmons, N. W. Hengartner, S. Singh, M. Zhernenkov, F. Y. Bruno, J. Santamaria, A. Brinkman, M. Huijben, H. J. A. Molegraaf, J. de la Venta, and I. K. Schuller, *Phys. Rev. Lett.* **107**, 217201 (2011).

³⁰See supplementary material at <http://dx.doi.org/10.1063/1.4938131> for details on the characterization of the Cr/MgO interface and of Cr growth process, along with precisions on the modelling of the PNR data.

³¹G. Gewinner, J. C. Peruchetti, A. Jaéglé, and R. Pinchaux, *Phys. Rev. B* **27**, 3358 (1983).

³²A. M. Bataille, V. Auvray, C. Gatel, and A. Gukasov, *J. Appl. Cryst.* **46**, 726 (2013).

³³E. W. Fenton, *Phys. Rev. Lett.* **45**, 736 (1980).

³⁴M. O. Steinitz, E. Fawcett, C. E. Burleson, J. A. Schaefer, L. O. Frishman, and J. A. Marcus, *Phys. Rev. B* **5**, 3675 (1972).

³⁵M. O. Steinitz, D. A. H. Pink, and D. A. Tindall, *Phys. Rev. B* **15**, 4341 (1977).

³⁶S. A. Werner, A. Arrott, and H. Kendrick, *Phys. Rev.* **155**, 528 (1967).

³⁷E. Kunnen, K. Temst, V. V. Moshchalkov, Y. Bruynseraede, S. Mangin, A. Vantomme, and A. Hoser, *Physica B* **276**, 738 (2000).

³⁸M.-A. Leroy, “Films minces épitaxiés de chrome pour l’électronique de spin: propriétés de volume: d interface,” Ph.D. thesis, Université de Lorraine (2013).